Cell Death and Differentiation (2013) 20, 97–107

www.nature.com/cdd

Noncanonical control of *C. elegans* germline apoptosis by the insulin/IGF-1 and Ras/MAPK signaling pathways

AJ Perrin[1,2], M Gunda[1], B Yu[1], K Yen[3], S Ito[1,2], S Forster[1], HA Tissenbaum[3,4] and WB Derry*[,1,2]

The insulin/IGF-1 pathway controls a number of physiological processes in the nematode worm *Caenorhabditis elegans*, including development, aging and stress response. We previously found that the Akt/PKB ortholog AKT-1 dampens the apoptotic response to genotoxic stress in the germline by negatively regulating the p53-like transcription factor CEP-1. Here, we report unexpected rearrangements to the insulin/IGF-1 pathway, whereby the insulin-like receptor DAF-2 and 3-phosphoinositide-dependent protein kinase PDK-1 oppose AKT-1 to promote DNA damage-induced apoptosis. While DNA damage does not affect phosphorylation at the PDK-1 site Thr350/Thr308 of AKT-1, it increased phosphorylation at Ser517/Ser473. Although ablation of *daf-2* or *pdk-1* completely suppressed *akt-1*-dependent apoptosis, the transcriptional activation of CEP-1 was unaffected, suggesting that *daf-2* and *pdk-1* act independently or downstream of *cep-1* and *akt-1*. Ablation of the *akt-1* paralog *akt-2* or the downstream target of the insulin/IGF-1 pathway *daf-16* (a FOXO transcription factor) restored sensitivity to damage-induced apoptosis in *daf-2* and *pdk-1* mutants. In addition, *daf-2* and *pdk-1* mutants have reduced levels of phospho-MPK-1/ERK in their germ cells, indicating that the insulin/IGF-1 pathway promotes Ras signaling in the germline. Ablation of the Ras effector *gla-3*, a negative regulator of *mpk-1*, restored sensitivity to apoptosis in *daf-2* mutants, suggesting that *gla-3* acts downstream of *daf-2*. In addition, the hypersensitivity of *let-60*/Ras gain-of-function mutants to damage-induced apoptosis was suppressed to wild-type levels by ablation of *daf-2*. Thus, insulin/IGF-1 signaling selectively engages AKT-2/DAF-16 to promote DNA damage-induced germ cell apoptosis downstream of CEP-1 through the Ras pathway.
Cell Death and Differentiation (2013) **20,** 97–107; doi:10.1038/cdd.2012.101; published online 31 August 2012

The response of cells to genotoxic stress requires integration of multiple pro-survival and pro-death signals. The growth factor-responsive kinase Akt, a target of phosphatidylinositol 3-kinase (PI3K) signaling, functions as a key node in this integration strategy.[1] By antagonizing pro-death pathways, Akt can effectively dampen pro-apoptotic signaling and ensure the survival of mammalian cells under stress.[2] Moreover, chemo- and radiotherapy has been shown to induce Akt activity,[3] which has a significant effect on resistance to therapy in Akt-expressing tumors.[4] Therefore, it is important to understand the mechanism(s) underlying the regulation of Akt in response to DNA damage, especially in light of the large number of cancers – including breast, colon, ovarian and prostate – that upregulate its oncogenic function.[1]

During *C. elegans* larval development, the PI3K pathway, composed of the insulin/IGF-1 receptor tyrosine kinase (InsR) DAF-2, the PI3K AGE-1 and the 3-phosphoinositide-dependent protein kinase PDK-1, controls the redundant activities of AKT-1 and AKT-2 on the forkhead transcription factor DAF-16 (Figure 1a;[5,6]). Phosphorylation of DAF-16 by AKT-1/AKT-2 prevents the translocation of DAF-16 into the nucleus and the subsequent induction of genes required for dauer entry,[7] lifespan[8,9] and stress response.[10] Although no distinct biological functions have been ascribed to AKT-1 and AKT-2, we previously showed that they regulate DNA damage-induced germ cell apoptosis from genetically separable pathways.[11] Whereas AKT-1 dampens the transcriptional activity of the p53 family member CEP-1, AKT-2 functions independently or downstream of CEP-1.

Here, we asked whether canonical signals upstream and downstream of AKT-1/AKT-2 regulate germline apoptosis in response to genotoxic stress. Unexpectedly, we observed complex regulation of germline apoptosis by the PI3K pathway independent of AKT-1 and the p53-like protein CEP-1. Rather than a positive acting cascade of signals through DAF-2-AGE-1-PDK-1 (Figure 1a), we found that the DAF-2 receptor tyrosine kinase and PDK-1 promote, rather than inhibit, damage-induced germ cell apoptosis. We found that DAF-2 and PDK-1 promote germline apoptosis through AKT-2 and DAF-16. Furthermore, we present evidence that insulin/IGF-1 signaling promotes signaling through Ras to drive germ cell apoptosis *in vivo*.

[1]Developmental and Stem Cell Biology Program, The Hospital for Sick Children, Toronto, Ontario M5G 1L7, Canada; [2]Department of Molecular Genetics, University of Toronto, Toronto, Ontario, Canada; [3]Program in Gene Function and Expression, University of Massachusetts Medical School, Worcester, MA, USA and [4]Program in Molecular Medicine, University of Massachusetts Medical School, Worcester, MA, USA
*Corresponding author: WB Derry, Developmental and Stem Cell Biology Program, The Hospital for Sick Children, Toronto Medical Discovery Tower, 101 College Street West, Toronto, Ontario M5G 1L7, Canada. Tel: +416 813 7654/Extn 1829; Fax: +416 813 2212; E-mail: brent.derry@sickkids.ca
Keywords: *C. elegans*; PI3K; apoptosis; DNA damage; Ras
Abbreviations: Akt, serine/threonine-specific protein kinase (also known as Protein Kinase B or PKB); IGF-1, Insulin-like growth factor 1; InsR, insulin receptor; PI3K, phosphatidylinositol 3-kinase; IR, ionizing radiation; L4, forth larval stage; MAPK, mitogen activated protein kinase; Ras, RAS protooncogene; PDPK1, 3–phosphoinositide-dependent protein kinase-1; RNAi, RNA interference; TORC2, target of rapamycin complex 2
Received 06.2.12; revised 22.6.12; accepted 08.7.12; Edited by E Baehrecke; published online 31.8.12

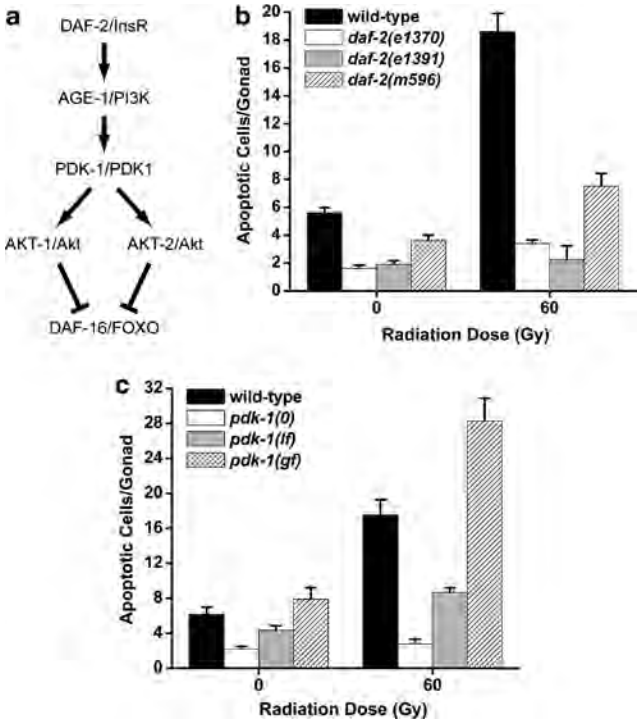

Figure 1 PI3K signaling promotes DNA damage-induced germ cell apoptosis. (**a**) The PI3K pathway in *C. elegans*. (**b** and **c**) *C. elegans* PI3K signaling components, *daf-2* and *pdk-1*, are required for damage-induced apoptosis. L4-stage worms were treated with IR and shifted to 25°C. Germ cell apoptosis was quantified 24 h later. *pdk-1(0) = pdk-1(sa680)*, *pdk-1(lf) = pdk-1(sa709)*, *pdk-1(gf) = pdk-1 (mg142)*. Error bars represent the S.E.M. from at least three independent experiments. At least ten animals were examined in each experiment

Results

PI3K signaling promotes DNA damage-induced germ cell apoptosis. Since ablation of the *C. elegans Akt* homolog, *akt-1*, sensitizes worm germ cells to ionizing radiation (IR)-induced apoptosis,[11] loss-of-function (lf) mutations in *daf-2*/InsR, *age-1*/PI3K and *pdk-1*/*PDPK1* should exhibit hypersensitivity to DNA damage-induced germ cell apoptosis. To examine this directly, we grew *daf-2(e1370)* lf mutant larvae to the L4 stage at the permissive temperature (15°C), exposed the worms to IR and then inactivated *daf-2* by temperature-shift to 25°C. After 24 h at the restrictive temperature, we quantified the number of apoptotic germ cells that formed. Surprisingly, damage-induced apoptosis was strongly suppressed in the germline of *daf-2(lf)* mutants when compared with wild-type (Figure 1b). Because this contradicted the weak anti-apoptotic role previously reported for *daf-2* in the worm germline,[12,13] we examined two additional alleles of *daf-2* (Figure 1b) and ablated *daf-2* by RNA interference (RNAi) (see below). Even though the *e1370, e1391* and *m596* alleles affect distinct regions of the *daf-2* locus,[14] all three mutations caused strong resistance to apoptosis. We also quantified IR-induced apoptosis in *daf-2(e1370)* mutants grown at 20°C, where only 15% of larva form dauers, and found that resistance to DNA damage was preserved (see Figure 4b) but not at the permissive temperature of 15°C (not shown). We conclude that *daf-2* is required to promote damage-induced germline apoptosis independent of its function in dauer development.

The unexpected pro-apoptotic role for *daf-2* in the germline prompted us to examine whether other components of the PI3K pathway were also required for IR-induced apoptosis. Loss of *age-1*/PI3K and *pdk-1*/*PDPK1* also caused strong resistance to apoptosis (Figure 1c and data not shown) and a kinase-independent gain-of-function (gf) mutation in *pdk-1*[5] caused hypersensitivity to DNA damage-induced germ cell apoptosis (Figure 1c). None of the insulin/PI3K pathway mutants had detectable changes in somatic cell apoptosis in developing embryos (data not shown).

Because it was possible that defects in germline proliferation could account for the resistance to apoptosis observed in *daf-2*, *age-1* and *pdk-1(lf)* mutants, we quantified germ cell numbers in these mutants. Under conditions identical to those used in our apoptosis assays, we detected a maximum 20% decrease in germ cell number in *daf-2(lf)* and *pdk-1(lf)* mutants and no change in *pdk-1(gf)* mutants compared with wild-type controls (Supplementary Table S1). The subtle decrease in germ cell numbers is insufficient to account for the ~80% reduction in damage-induced apoptosis in *daf-2* and *pdk-1(lf)* mutants (Figure 1). Although *age-1* mutants were also resistant to damage-induced apoptosis, we noticed strong proliferation defects in the germlines of *age-1(mg44)* null mutants (data not shown) and therefore excluded this gene from further analysis.

To determine if *daf-2* and *pdk-1* were also required for physiological germline apoptosis, we ablated these genes in *ced-1(e1735)* mutants, which are defective in the engulfment of cell corpses and therefore increase the sensitivity of detecting subtle changes in apoptosis.[15] The number of physiological germ cell corpses in *ced-1* mutants was essentially unchanged when either *daf-2* was ablated by RNAi or *pdk-1* function reduced by the *sa709* allele (Supplementary Figure S1). Therefore, we conclude that *daf-2* and *pdk-1* function specifically to promote DNA damage-induced apoptosis in the worm germline.

***daf-2*/InsR and *pdk-1*/*PDPK1* function independently of *cep-1*/p53 and *akt-1*/*Akt*.** The antagonistic roles *daf-2/pdk-1* and *akt-1* in germ cell apoptosis caused us to question the organization of the worm PI3K pathway in the context of DNA damage. If the pathway were linear in structure, as in the control of dauer arrest (Figure 1a), then null mutations in *akt-1* should be able to restore sensitivity of *daf-2(lf)* and *pdk-1(lf)* mutants to apoptosis. Because the somatic defects of *daf-2*; *akt-1* compound mutants made quantifying germ cell apoptosis difficult, we instead inhibited *daf-2* using RNAi in *akt-1(ok525)* null mutants. Surprisingly, loss of *akt-1* was unable to revert the resistance of *daf-2(RNAi)* germ cells to IR-induced apoptosis (Figure 2a). This suggested that *daf-2* functioned either downstream or independently, but not upstream of, *akt-1* in response to DNA damage. Because this result contradicted contemporary models of PI3K signaling,[1] we next asked if ablation of *akt-1* could restore sensitivity to apoptosis in *pdk-1(lf)* mutants. Strikingly, *akt-1(0); pdk-1(lf)* double mutant worms were as resistant to IR-induced germ cell apoptosis as *pdk-1(lf)* mutants (Figure 2b).

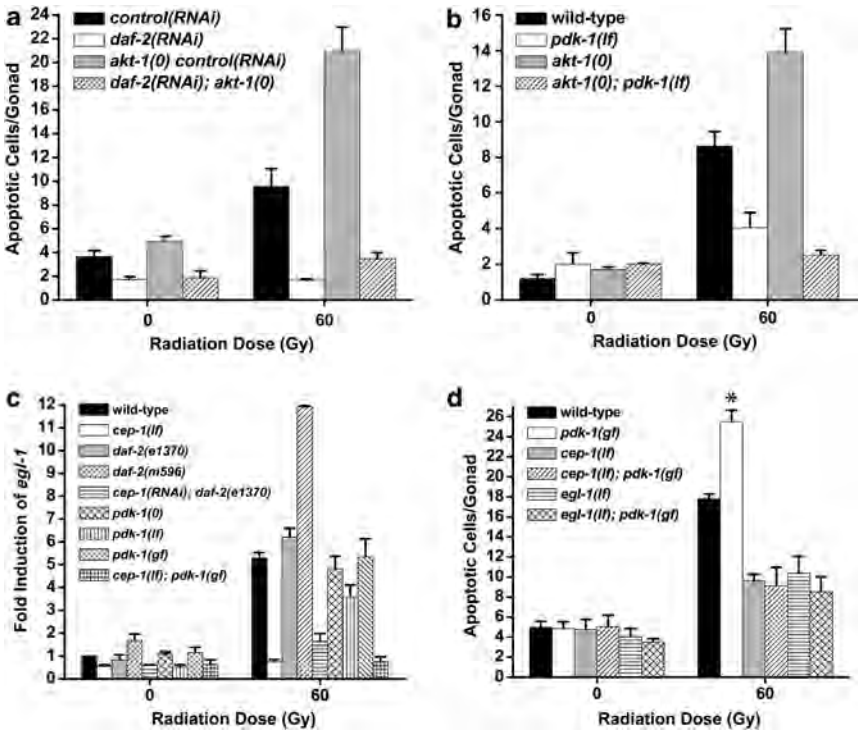

Figure 2 *daf-2* and *pdk-1* do not function upstream of *akt-1* or *cep-1*. (**a**) Young adults were irradiated, incubated at 20°C for 24 h and apoptosis was quantified as in Figure 1. RNAi was performed in the *rrf-3(pk1426)* background. *akt-1(0)* = *akt-1(ok525)*. (**b**) L4 stage worms were treated as in (**a**). *pdk-1(lf)* = *pdk-1(sa709)*, *akt-1(0)* = *akt-1 (ok525)*. (**c**) L4 stage worms were treated with IR, incubated at 25°C for 24 h and total RNA was isolated. *egl-1* transcript was quantified by Real-Time PCR using *tbg-1* as an internal standard. *cep-1(lf)* = *cep-1(gk138)*, *pdk-1(0)* = *pdk-1(sa680)*, *pdk-1(lf)* = *pdk-1(sa709)*, *pdk-1(gf)* = *pdk-1(mg142)*. (**d**) L4 stage worms were treated with IR and germ cell apoptosis was quantified after 24 h at 25°C. *pdk-1(gf)* = *pdk-1(mg142)*, *cep-1(lf)* = *cep-1(gk138)*, *egl-1(lf)* = *egl-1(n1084n3082)*. Error bars as in Figure 1. *$P<0.001$ *versus* wild-type

As loss of *pdk-1* fully suppressed damage-induced germ cell apoptosis in *akt-1(0)* mutants, it is likely that *pdk-1* (like *daf-2*) functions downstream or independently of *akt-1* in the DNA damage response. This was supported by the lack of a checkpoint phenotype for *daf-2* and *pdk-1*. In the *C. elegans* germline, the 9-1-1 checkpoint (encoded by *hpr-9*, *mrt-2* and *hus-1*) and *clk-2*, sense and relay DNA damage signals to *cep-1*.[16–18] These sensors are required to promote apoptosis of germ cells in the pachytene region by activating CEP-1 and elicit a transient cell cycle arrest of mitotically proliferating cells in the distal region of the gonad in response to genotoxic stress.[19] We observed a robust cell cycle arrest in the distal mitotic zone of *daf-2* and *pdk-1* mutant germlines treated with IR that was identical to wild-type controls (data not shown). Therefore, we conclude that *daf-2* and *pdk-1* do not function as DNA damage sensors upstream of *akt-1*.

Downstream of the DNA damage checkpoint, AKT-1 negatively regulates the transcriptional activity of CEP-1, which activates expression of the BH3-only protein EGL-1.[18] We reasoned that if *daf-2* and *pdk-1* functioned downstream of *akt-1*, but upstream of *cep-1*, their loss should impede the transcriptional function of CEP-1. To test this directly, we treated multiple alleles of *daf-2* and *pdk-1* with IR and assessed CEP-1 transcriptional activity by quantification of *egl-1* mRNA. While DNA damage caused *egl-1* transcript levels to increase approximately fivefold over unirradiated wild-type worms, *egl-1* was induced to the same levels in *daf-2(e1370)* mutants and approximately twice this level in *daf-2(m596)* mutants (Figure 2c). In addition, *egl-1* induction in *pdk-1(sa680)*, *pdk-1(sa709)* and *pdk-1(mg142)* mutants was not substantially different than in wild-type controls (Figure 2c). These results indicate that *daf-2* and *pdk-1* act downstream or independent of *cep-1* and *akt-1* to promote damage-induced germ cell apoptosis.

Despite *pdk-1* not being required for CEP-1 transcriptional function (Figure 2c), we wondered whether functional *cep-1* was required for *pdk-1* to kill damaged germ cells. To address this, we generated *cep-1(gk138); pdk-1(mg142)* double mutants and assessed their response to IR. If the *pdk-1 (mg142)* gf allele can promote apoptosis independently or downstream of *cep-1*, we would predict to observe increased apoptosis in *cep-1(lf)*, *pdk-1(gf)* double mutants relative to *cep-1(lf)*. Surprisingly, germ cell apoptosis in *cep-1(lf); pdk-1 (gf)* double mutants was suppressed to the levels seen in *cep-1(lf)* single mutants (Figure 2d). Consistent with this, *egl-1* is also required for *pdk-1* to promote/enhance apoptosis, as *egl-1(lf); pdk-1(gf)* double mutants have similar numbers of corpses as *egl-1(lf)* single mutants treated with IR (Figure 2d). Thus, *pdk-1* modulates the magnitude of apoptosis signaling independently or downstream of *cep-1*/*egl-1*.

AKT-1/Akt phosphorylation is not affected by DNA damage. Through canonical PI3K signaling the activity of Akt proteins is tightly controlled by phosphorylation on two key residues - Thr308 and Ser473 in human Akt1.[20] These phosphorylation events, mediated by PDPK1 at Thr308 and

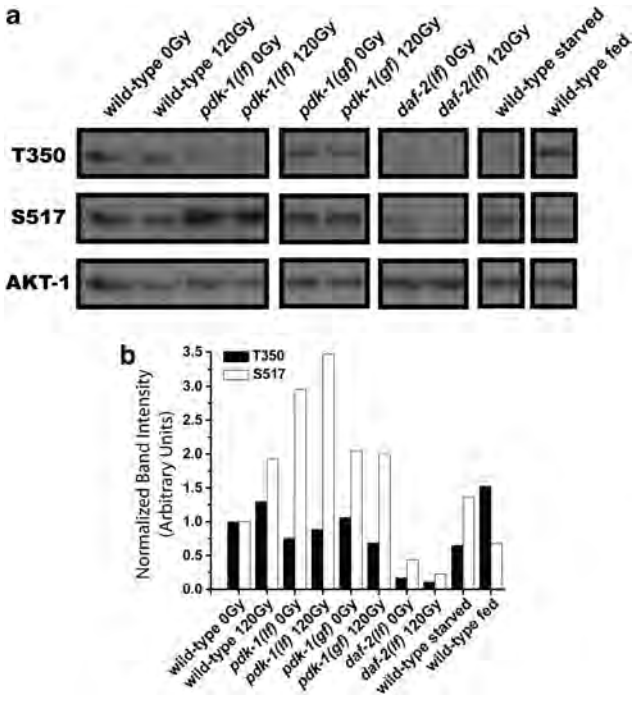

Figure 3 AKT-1 is regulated independently of Thr350 phosphorylation. (**a**) Worms were irradiated and AKT-1 was immunoprecipitated as described in Materials and Methods. All samples were run on the same gel, transferred to PVDF and probed for phospho-T350, S517 and total AKT-1. *pdk-1(lf) = pdk-1(sa709)*; *pdk-1(gf) = pdk-1(mg142)*; *daf-2(lf) = daf-2(e1370)*. (**b**) The intensity of T350 and S517 in each lane was quantified using ImageJ and normalized to total AKT-1. The normalized intensity of each band was expressed relative to wild-type unirradiated. Data represent the average of two experiments

TORC2 (mammalian target of rapamycin complex 2) at Ser473,[21] ensure optimal catalytic activity of the kinase.[20] To investigate the phosphorylation state of AKT-1 we raised two mono-specific polyclonal antisera against different regions of AKT-1 (Supplementary Figure S2), immunoprecipitated endogenous protein from worm lysates and probed blots with phospho-specific antibodies to T350 (homologous to T308) and S517 (homologous to S473) previously generated.[22] In the absence of IR both T350 and S517 were phosphorylated, consistent with tonic insulin/IGF-1 signaling under normal growth conditions. Consistent with our genetic data suggesting noncanonical regulation of AKT-1, radiation did not dramatically alter the phosphorylation state of T350/T308 in the wild-type compared to the unirradiated controls (Figure 3a). Interestingly, there was a doubling in the levels of S517 phosphorylation in wild-type animals treated with IR, suggesting that AKT-1 might be regulated at this site in response to DNA damage (Figure 3b). In *pdk-1(lf)* worms, only a modest reduction in T350 phosphorylation was observed (Figure 3a). Since we did not observe a robust upregulation in T350 phosphorylation after IR in *pdk-1(gf)* mutants, it is unlikely that PDK-1 functions to control AKT-1 phosphorylation in response to DNA damage (Figure 3b). Loss of *pdk-1* did however result in a significant ($\sim$ 3-fold) upregulation of AKT-1 at S517 in the absence of irradiation (Figures 3a and b). This likely reflects conservation of a negative feedback loop centered on TORC1 inhibition of PI3K.[23] Loss of *daf-2* completely abrogated AKT-1 T350 and S517 phosphorylation (Figure 3), indicating that *daf-2* is essential for basal AKT-1 phosphorylation and that DAF-2 might also promote basal AKT-1 phosphorylation independently of PDK-1.

***daf-2*/InsR and *pdk-1*/*PDPK1* promote germ cell apoptosis through the core cell death pathway.** The ability of CEP-1 to drive *egl-1* transcription in the absence of either *daf-2* or *pdk-1*, combined with the inability of *akt-1(0)* mutations to restore apoptosis in *daf-2* and *pdk-1* mutants, suggested that *daf-2* and *pdk-1* could function in the same *cep-1*-independent pro-apoptotic pathway. If this were true, then *pdk-1(gf)* mutations should be able to revert the resistance of *daf-2(lf)* mutants to DNA damage. As shown in Figure 4a, increased PDK-1 activity could not revert the resistance of *daf-2(e1370)* mutants to DNA damage, consistent with previous work showing that the *mg142* allele does not suppress *daf-2(e1370)* in the dauer pathway.[5]

To further investigate how *daf-2* and *pdk-1* regulated apoptosis, we examined their genetic interactions with components of the core apoptosis pathway. Downstream of *egl-1*, CED-9/Bcl2 negatively regulates CED-4/Apaf1-dependent CED-3/Caspase activation.[24] To determine where *daf-2* and *pdk-1* functioned with respect to *ced-9*, we assessed whether loss of either *daf-2* or *pdk-1* could suppress the excessive germ cell apoptosis seen in *ced-9* null mutants. Informatively, loss of *daf-2* did not alter the levels of germ cell apoptosis in *ced-9(n2812)* null mutants, whereas loss of *pdk-1* reduced apoptosis to wild-type levels in *ced-9(0)* (Figures 4b and c). As loss of *daf-2* or *pdk-1* had identical effects on germline proliferation (Supplementary Table S1), these results suggested that *daf-2* functions upstream, or independently of *ced-9*, while *pdk-1* might also contribute pro-apoptotic signals in parallel to *ced-9*. Immunostaining of dissected germlines did not reveal any detectable differences in levels or localization of endogenous CED-9 protein in *daf-2* mutants compared with wild-type controls (Supplementary Figure S3). Furthermore, *pdk-1* does not function solely downstream of *ced-9* in the apoptotic cascade, as *pdk-1(lf)* could not revert the sterility of maternally rescued *ced-9(0)* homozygotes (Supplementary Table S2). On the other hand, the *ced-4(n1162)* null mutation was able to completely suppress the hypersensitivity of *pdk-1(gf)* mutant germ cells to IR (Figure 4d), suggesting that *pdk-1* controls apoptosis upstream of *ced-4*. *pdk-1* does not appear to regulate the localization of CED-4, as we did not detect any changes in the germline localization of CED-4 in response to IR in wild-type animals nor in *pdk-1* mutants (Supplementary Figure S4A). We also did not detect any changes in absolute CED-4 protein levels in either genetic background (Supplementary Figure S4B). This suggested that defects in CED-4 localization or protein levels do not underlie the alterations of apoptosis in *pdk-1* mutants.

The histone deacetylase SIR-2.1 has been shown to change localization in response to DNA damage and it has been suggested that SIR-2.1 regulates CED-4 localization to promote DNA damage-induced germ cell apoptosis.[25] Therefore, we assessed whether alterations in *pdk-1* function affected the localization of SIR-2.1 in response to DNA

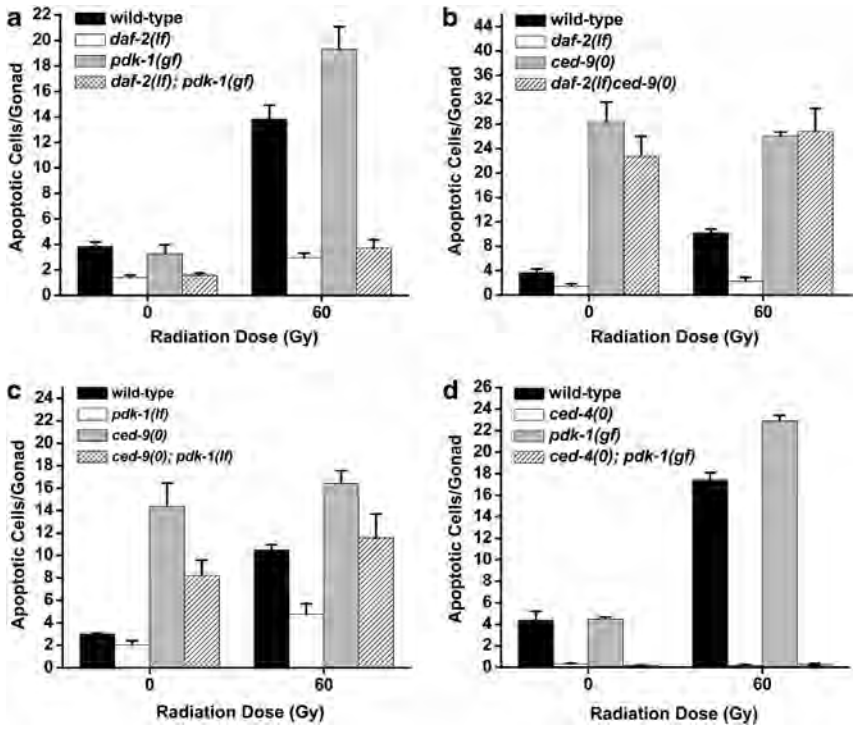

Figure 4 *daf-2* and *pdk-1* independently regulate the core apoptosis pathway. L4 stage (**a**, **c**, **d**) or young adult (**b**) worms were irradiated and germ cell apoptosis was quantified after 24 h at 20°C (**b** and **c**), or 25°C (**a** and **d**). Owing to the somatic effects of *daf-2* and *pdk-1* loss on the visibility of the germline in *daf-2ced-9* and *ced-9; pdk-1* double mutants, we found it necessary to perform these two epistasis experiments at slightly different developmental time points (48 h post-L4 in the case of *daf-2ced-9* and 24 h post-L4 for *ced-9; pdk-1*). As worms age from L4 to young adult, the germline continues to expand in size and this is reflected by a small increase in basal levels of apoptosis. Therefore, the absolute levels of apoptosis seen in *ced-9(0)* mutants in the *daf-2ced-9* experiment is greater than that seen in the *ced-9; pdk-1* experiment. This should not alter our interpretation of epistasis, however, as loss of *pdk-1* exerts an ~1.3-fold greater suppressive effect on *ced-9(0)* than does loss of *daf-2*. *daf-2(lf)* = *daf-2 (e1370)*, *ced-9(0)* = *ced-9(n2812)*, *ced-4(0)* = *ced-4(n1162)*. Error bars as in Figure 1

damage. SIR-2.1 was reduced in the nuclei of dying cells of all genotypes tested and its localization in non-dying cells was unaffected by *pdk-1* (Supplementary Figure S4C). Because excessive apoptosis in *pdk-1(gf)* mutants is not due to delayed or defective clearance of dying cells (Supplementary Table S3), we conclude that *pdk-1* requires the core apoptotic pathway to promote apoptosis but likely functions independently of *sir-2.1*. In addition, *pdk-1* may have *daf-2*-independent functions that regulate *ced-4* by a novel mechanism.

***daf-2*/InsR and *pdk-1*/*PDPK1* promote apoptotic signals through *akt-2* and *daf-16*.** Previously, we showed that while both *akt-1* and *akt-2* negatively regulate IR-induced germline apoptosis, *akt-2*, unlike *akt-1*, functions downstream of CEP-1.[11] As *daf-2(lf)* mutants are resistant to damage-induced germline apoptosis but activate CEP-1 transcription of *egl-1* in response to IR (Figure 2c), we next asked if DAF-2 transmits pro-apoptotic signals selectively through AKT-2. In contrast with *daf-2(lf)*; *akt-1(lf)* double mutants (Figure 2a), we observed that ablation of *akt-2* using the *ok393* deletion allele in *daf-2(lf)* worms restored germline apoptosis to nearly wild-type levels after treatment with IR (Figure 5a). Because sensitivity to apoptosis was not restored to the same levels as that observed in *akt-2(0)* single mutants, we conclude that *daf-2* transmits apoptotic signals through *akt-2* and possibly through a parallel pathway that does not require *akt-1*.

As the best characterized downstream target of the insulin signaling pathway in *C. elegans* is the forkhead transcription factor DAF-16, we next asked whether ablation of *daf-16* could restore apoptosis sensitivity to *daf-2(lf)* mutants. Similar to *daf-2(lf)*; *akt-2(0)* double mutants, sensitivity to apoptosis was restored when *daf-16* was ablated by RNAi in *daf-2(lf)* mutants (Figure 5a). We observed the same effect in *daf-2(lf)*; *daf-16(mgDf47)* double mutants (data not shown). The restoration of apoptosis in *daf-2(lf)* mutants by loss of *daf-16* was not due to hyperproliferation of the germline, as the double mutants had similar numbers of germ cells as wild-type animals (Supplementary Table S1). Finally, we created a triple mutant in which *akt-2* and *daf-16* were ablated with *daf-2* and observed similar levels of apoptosis as *daf-2*; *akt-2* or *daf-2*; *daf-16* double mutants, providing genetic evidence that *akt-2* regulates *daf-2*-dependent apoptosis through *daf-16* (Figure 5a). In addition, resistance to apoptosis in *pdk-1(sa709)* mutants was restored to wild-type levels by ablation of *akt-2* or *daf-16* (Figures 5b and c), suggesting that the insulin/IGF-1 pathway selectively recruits AKT-2 to transduce pro-apoptotic signals from DAF-2. Interestingly, the serum and glucocorticoid kinase SGK-1 completely suppresses PDK-1-dependent damage-induced germline apoptosis, but unlike DAF-2 does not act through DAF-16 (Figure 5d).

***daf-2*/InsR promotes DNA damage-induced germline apoptosis through Ras/MAPK signaling.** The Ras

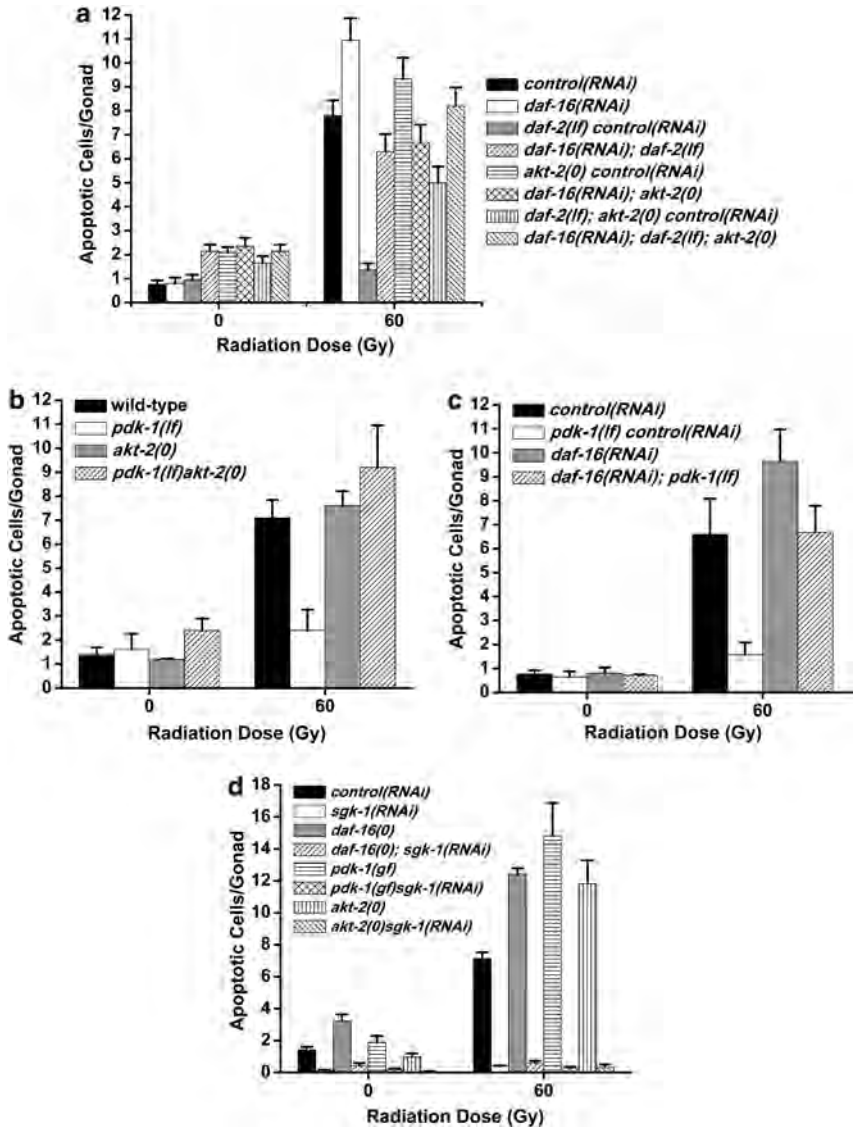

Figure 5 *daf-2* promotes damage-induced germ cell apoptosis via *akt-2* and *daf-16*. (**a–d**) L4 stage worms were transferred to fresh RNAi plates, treated with IR and germ cell apoptosis quantified after 24 h at 20°C. *akt-2(0)* = *akt-2(ok393)*, *daf-2(lf)* = *daf-2(e1370)*, *daf-16(0)* = *daf-16(mgDf47)*, *pdk-1(lf)* = *pdk-1(sa709)*. Because the kinetics underlying apoptosis are increased at higher temperatures, the number of apoptotic cells observed in assays conducted at 20°C is lower than that seen at 25°C (see Figure 1). This reflects the temperature-dependent effects on the apoptotic process itself; the relative difference between genotypes is usually independent of this. Control RNAi experiments were carried out in wild-type (N2) animals

signaling pathway is required for germ cells to exit the pachytene stage of meiosis I,[26] which makes them competent to undergo physiological apoptosis.[27] The Ras/MAP kinase pathway also promotes DNA damage-induced germ cell apoptosis by *cep-1*-dependent and *cep-1*-independent mechanisms.[28,29] Given that insulin/IGF-1 has been shown to promote Ras/MAPK signaling in *C. elegans* vulval development and lifespan,[30,31] we wondered if they also cooperate in promoting germline apoptosis. Using antibodies to phosphorylated ERK, which has been shown to cross-react with phospho-MPK-1 in *C. elegans*,[29] we stained germlines isolated from wild-type, *daf-2(lf)* and *pdk-1(lf)* mutants treated with IR (Figure 6). We confirmed the pattern of phospho-MPK-1 staining previously reported in germlines before and after IR treatment,[29] but observed a substantial reduction in *daf-2(lf)* mutants compared with wild-type controls before and after IR (Figures 6c and d). We also observed a reduction in staining of *pdk-1(lf)* mutant germlines after IR, but this was not as pronounced as *daf-2(lf)* mutants (Figures 6e and f). To confirm that *pdk-1* does indeed function upstream of *mpk-1*, we inhibited *mpk-1* by RNAi in *pdk-1(gf)* mutants and found that loss of *mpk-1* was able to completely suppress the hypersensitivity to apoptosis seen in *pdk-1(gf)* single mutants (Figure 6i). These results indicate that insulin/IGF-1 signaling promotes phosphorylation of MPK-1 in the germline.

To determine if Ras/MAPK signaling could restore sensitivity to apoptosis in the absence of *daf-2*, we used the Ras gf allele, *let-60(ga89)*, previously shown to cause hypersensitivity to IR-induced germline apoptosis.[29] Ablation of *daf-2* in *let-60(ga89)* mutants reduced germline apoptosis to similar levels as wild-type after IR (Figure 6j). This suggested that

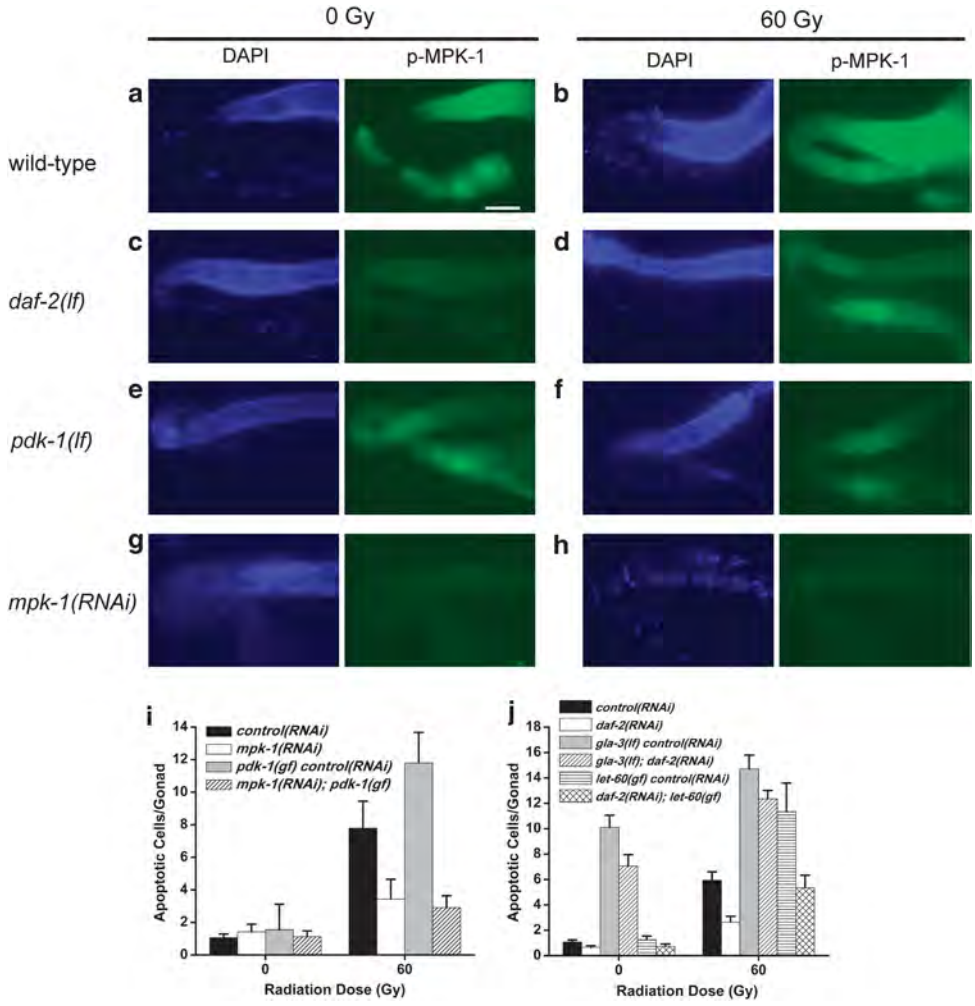

Figure 6 *daf-2* and *pdk-1* promote germline apoptosis through Ras/MAPK signaling. (**a–f**) Phospho-MPK-1 and DAPI staining in germlines of the indicated genotype before and after irradiation. (**g–h**) *mpk-1(RNAi)* negative controls in the absence and presence of IR. (**i**) Loss of *mpk-1* in *pdk-1(mg142)* mutants suppresses excessive apoptosis. (**j**) Ablation of *daf-2* by RNAi suppresses IR-induced germ cell apoptosis to wild-type levels in *let-60(ga89)* gf mutants, but does not suppress apoptosis in *gla-3(op216)* mutants. Worms were irradiated as in Figure 1 and incubated at 20°C for 24 h. Error bars as in Figure 1

DAF-2 is required to promote or sustain amplified Ras signaling but is dispensable for basal Ras signaling. Consistent with the insulin/IGF-1 pathway promoting activated Ras/MAPK signaling, we found that ablation of *daf-2* by RNAi suppressed the multivulva phenotype of *let-60(n1024)* gf mutants from 75 to 7% (data not shown), in agreement with previous observations.[30] We also examined germline apoptosis in *gla-3(op312)* mutants, which are hypersensitive to IR-induced germ cell apoptosis through activation of MPK-1.[28] While *daf-2(RNAi)* completely suppressed IR-induced apoptosis, we observed similar levels of apoptosis when *daf-2* was ablated in the *gla-3* mutants compared with *gla-3* controls (Figure 6j). Thus, we concluded that insulin/IGF-1 signaling promotes germline apoptosis through Ras/MAPK signaling, upstream of *gla-3*.

Distinct tissue expression requirements underlie damage-dependent re-arrangements in the PI3K pathway. Because *daf-2* is known to regulate both dauer arrest[32] and aging non-autonomously,[33] we were interested in knowing whether the genetic independence of *daf-2* and *akt-1* could be explained by different tissue requirements. Mutations in *rrf-1* and *ppw-1* selectively disable RNAi in the soma or the germline, respectively,[34,35] but do not affect damage-induced apoptosis (Figure 7).[36] *akt-1(RNAi)* caused hypersensitivity to damage-induced apoptosis, and this effect was preserved in *rrf-1(0)* mutants, which are only competent for germline RNAi (Figure 7a). Conversely, *akt-1(RNAi)* did not sensitize *ppw-1(lf)* mutant germ cells to DNA damage (Figure 7a). We also took advantage of an extrachromosomal array that expressed *akt-1* in a tissue-specific manner and found that expression of *akt-1* in the soma of *akt-1(0)* mutants was unable to revert sensitivity to DNA damage-induced apoptosis (Figure 7c). We conclude that *akt-1* is required cell autonomously in the germline to regulate cell death.

Unlike *akt-1*, we found that *daf-2(RNAi)* could not suppress apoptosis in either *rrf-1* or *ppw-1* mutants (Figure 7b), suggesting that *daf-2* is required in both the soma and

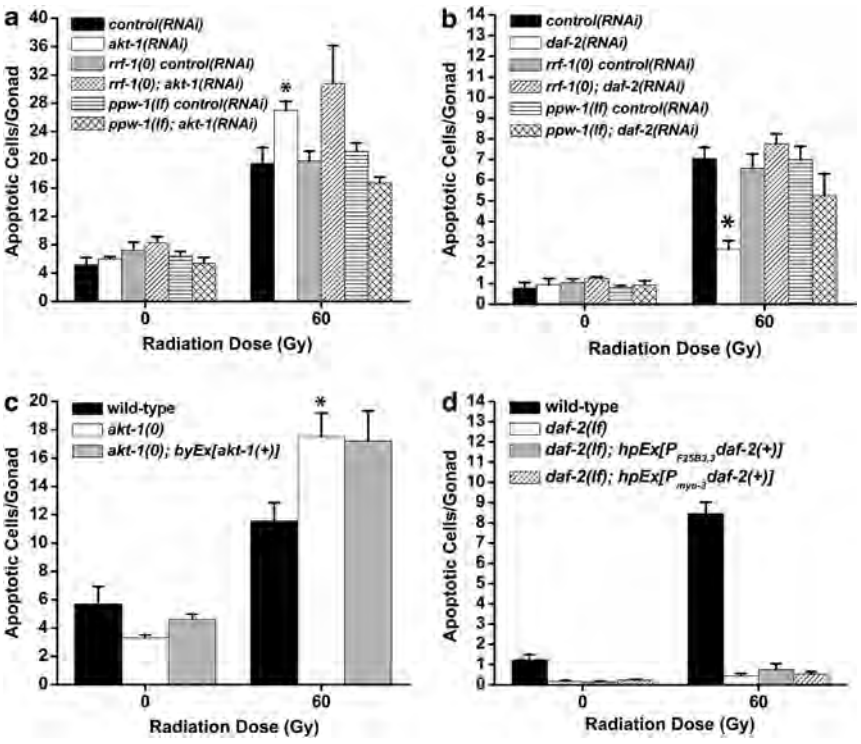

Figure 7 *akt-1* and *daf-2* function from different tissues to regulate damage-induced germ cell apoptosis. (**a**) Young adult worms were transferred to fresh RNAi plates, treated with IR and germ cell apoptosis was quantified after 24 h at 20°C. *rrf-1* and *ppw-1* are required for RNAi in the soma and germline, respectively. *rrf-1(0) = rrf-1(pk1417)*, *ppw-1(lf) = ppw-1(pk1425)*. Error bars as in Figure 1. **P* < 0.05 *versus control(RNAi)*. (**b**) L4-stage worms were transferred to fresh RNAi plates, treated with IR and germ cell apoptosis was quantified after 24 h at 20°C. Error bars as in Figure 1. **P* < 0.01 *versus control(RNAi)*. (**c**) Young adult worms were treated with IR and germ cell apoptosis was quantified after 24 h at 20°C. *byEx[akt-1(+)]* is a high-copy extrachromosomal array that rescues the somatic Daf-c phenotype of *akt-1(ok525); akt-2(RNAi)* worms. *akt-1 (0) = akt-1(ok525)*. Error bars are as in Figure 1. **P* < 0.05 *versus* wild type. (**d**) L4-stage worms were transferred to fresh plates, treated with IR and germ cell apoptosis was quantified after 24 h at 20°C. *daf-2(lf) = daf-2(e1370)*, *hpEx[$P_{F25B3.3}$daf-2(+)] = hpEx792*, a high-copy array that expresses *daf-2* in the nervous system; *hpEx[P_{myo-3} daf-2(+)] = hpEx791*, a high-copy array that expresses *daf-2* in muscle. Error bars are as in Figure 1

germline to promote damage-induced germ cell apoptosis. Our tissue-specific RNAi experiments predict that when *daf-2* is expressed strictly in the soma it should not be able to rescue the resistance to apoptosis of *daf-2(lf)* mutants. This was indeed true when we expressed *daf-2(+)* from either the pan-neuronal *F25B3.3* promoter[37] or the muscle-specific *myo-3* promoter (Figure 7d). The tissue-specific requirements for *daf-2* and *akt-1* are consistent with our data placing *daf-2* and *akt-1* in independent genetic pathways and suggest that the alterations in the PI3K pathway could reflect functional compartmentalization that ensures context-specific PI3K pathway output.

Discussion

The PI3K-Akt signaling pathway generates a strong anti-apoptotic signal across phylogeny.[1] We have previously shown that *C. elegans* AKT-1 transmits an anti-apoptotic signal by negatively regulating the p53-like transcription factor CEP-1.[11] In this study, we sought to understand whether the worm insulin-IGF-1 pathway, like its mammalian counterpart, was important in regulating DNA damage-dependent AKT-1 function. Surprisingly, we found that components of the worm PI3K pathway upstream of *akt-1* opposed its anti-apoptotic function. While DAF-2 and PDK-1 normally activate the redundant functions of AKT-1 and AKT-2 to prevent worms from entering the dauer stage of development, we find that DAF-2 and PDK-1 selectively engage AKT-2, DAF-16/FOXO and the Ras/MAPK pathway to promote apoptosis of damaged germ cells. Our results also suggest the existence of AKT-2/DAF-16-independent apoptotic outputs downstream of DAF-2, revealing noncanonical fragmentation of the PI3K signaling axis and cross-talk with Ras signaling. Fragmentation of PI3K signaling could reflect the worm's ability to maximize flexibility of a single pathway for different biological functions. Thus, a simple signaling pathway can become far more robust than initially predicted, and previous studies had hinted at such functional flexibility in the PI3K pathway. For example, the *pdk-1-akt-1* cassette is conditionally split in the regulation of lifespan, but not dauer arrest in the worm,[38,39] and studies in mouse have found that separation of Akt and PDPK1 function occurs in different tissues of the central nervous system.[40] Our previous study hinted at distinct roles for AKT-1 and AKT-2 in the control of germline apoptosis that we have advanced into a mechanistic framework here. While AKT-1 modulates CEP-1 transcriptional activity, we show that the CEP-1-independent apoptotic activity of AKT-2 acts through the canonical PI3K pathway and its downstream target DAF-16. In *C. elegans* dauer development and lifespan control *akt-1* and *akt-2* function redundantly,[6,41] but we have

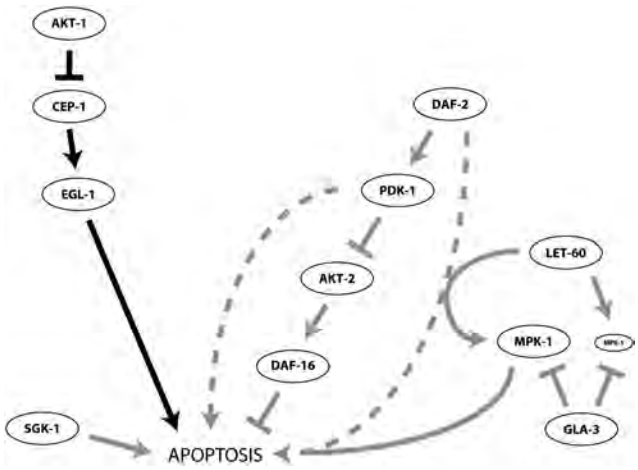

Figure 8 Model depicting the regulation of DNA damage-induced germ cell apoptosis by *C. elegans* PI3K pathway components. DAF-2 promotes apoptosis independently of AKT-1 by selectively engaging AKT-2 to regulate DAF-16 (AKT-1 inhibits CEP-1 from within damaged germ cells). PDK-1 functions through CED-4 and at least partially through AKT-2/DAF-16 to promote apoptosis downstream of CEP-1 and EGL-1. Although PDK-1 cannot promote apoptosis in the absence of CEP-1 and EGL-1, both DAF-2 and PDK-1 are required for amplification of LET-60/Ras signals that promote MPK-1/ERK phosphorylation and increase damage-induced apoptosis in the germline. SGK-1 promotes damage-induced germ cell apoptosis independently of the canonical Insulin/IGF-1 pathway. Arrows indicate activation, cross-hatches inhibition

uncovered a novel role for AKT-2 in the regulation of DNA damage-induced germline apoptosis. Unlike the canonical PI3K pathway, where the AKT-1/2 kinases are activated by the upstream InsR-PI3K-PDPK1 module, our results indicate that these upstream components inhibit AKT-2 in response to genotoxic stress. Alternative PI3K pathway signaling also extends to disease processes such as cancer where, in the background of activated PI3K mutations, PDPK1-based signaling is directed away from Akt and instead target serum and glucocorticoid-inducible kinase 3 (SGK3) to drive proliferation and anchorage-independent cell growth.[42] Interestingly, we found that the *C. elegans* SGK homolog SGK-1, like DAF-2 and PDK-1, is required to promote damage-induced germ cell apoptosis, but through a DAF-16-independent mechanism (Figure 5d). Our work also provides important confirmation that parallel pathways collaborate to drive cell death in the worm germline. The inability of *pdk-1* to function without *cep-1* (Figure 2d) suggests that other *cep-1*-independent regulators – for example, *sir-2.1* and *kri-1* – could function in a pro-apoptotic network rather than a linear pro-death pathway.[25,36] This prompts a re-evaluation of the organization of pro-apoptotic signaling pathways and necessitates our consideration that conserved pathways could function in parallel to p53 to promote cell death in mammals. This may have implications in understanding why cancers contain multiple mutations in pro-death signaling pathways.

Because our genetic data argue for a novel manner of PI3K signaling in response to DNA damage (Figure 8), we suggest that AKT-1 activity in the germline is controlled independently of T350/T308 phosphorylation. It is possible that phosphorylation at S517/S473 could be more important for AKT-1 function in response to IR, as levels of this modification nearly doubled after IR in the wild type (Figure 3b). This is consistent with previous studies showing that S473 phosphorylation is important for the anti-apoptotic function of mammalian Akt.[43] As TORC2 is known to phosphorylate human Akt at S473,[21] it will be important to determine if worm TORC2 is responsible for the anti-apoptotic function of AKT-1. It is also possible that damage-specific regulation of AKT-1 could involve phosphorylation at other residues. Finally, damage-specific binding partners could facilitate proper function of AKT-1 in the absence of altered phosphorylation at the T350 and S517 sites.

Noncanonical PI3K signaling in the context of DNA damage, where *daf-2* and *pdk-1* function independently of *akt-1*, is not likely peculiar to *C. elegans*, as a recent study showed parallel signaling from the insulin and IGF-1 receptors (homologs of DAF-2) is required for apoptosis of preadipocytes upon serum withdrawal.[44] This suggests that the pro-apoptotic function of the insulin receptor family is conserved from worms to humans, and our results may have applicability in combating Akt-dependent cancers. Although PDK-1 bypasses AKT-1 in response to IR, it is unclear how PDK-1 regulates CED-4 in the germline. Because we could not detect any alteration in CED-4 nor SIR-2.1 protein localization or levels in the wild-type or in *pdk-1* mutants in response to IR (Supplementary Figure S4), it is possible that PDK-1 controls CED-4 by a less obvious mechanism. Future experiments are necessary to determine if such a model explains the role of *pdk-1* in *C. elegans* germline apoptosis.

Importantly, we demonstrate cross-talk between the PI3K and Ras signaling pathways in promoting damage-induced apoptosis. It has been suggested that Ras signaling is required for establishing competence of the germline to undergo apoptosis.[29] We suggest an alternative model in which noncanonical insulin/IGF-1 signaling selectively inhibits AKT-2/DAF-16 to amplify Ras signals above a threshold. It is unlikely that insulin/IGF-1 signaling is required for normal Ras signaling, as complete inhibition of the Ras pathway causes sterility by arresting germ cells at the pachytene stage of meiosis I.[26] We propose that reduced levels of phosphorylated MPK-1 in the germ cells of *daf-2* and *pdk-1* mutants is below the threshold required for amplifying oncogenic Ras signaling but not low enough to cause sterility. This is supported by the fact that the *daf-2* and *pdk-1* mutants are competent to complete meiosis and remain fertile at temperatures that prevent their germ cells from undergoing damage-induced apoptosis. In addition, ablation of *daf-2* reduced the somatic consequences of hyperactivated Ras by suppressing the multivulva phenotype of *let-60(gf)* mutants, but did not prevent formation of a single functional vulva in these animals (data not shown). Therefore, we propose a model in which noncanonical insulin/IGF-1 signaling is required to sustain hyperactivated Ras signaling (Figure 8). Understanding the molecular mechanisms by which these oncogenic pathways communicate should help identify more selective therapies for targeting cancers in which Ras and PI3K signaling cooperate to drive transformation and tumorigenesis.

Materials and Methods

***Caenorhabditis elegans* genetics.** Worms were maintained on NGM (nematode growth medium) plates seeded with *E. coli* OP50. Double mutants were constructed according to standard protocols. Alleles used in this study included: Linkage Group I – *ced-1(e1735)*, *cep-1(gk138)*, *gla-3(op312)*, *ppw-1(pk1425)*, *rrf-1(pk1417)*; Linkage Group II – *age-1(ag12)*, *age-1(hx546)*, *age-1(mg44)*, *rrf-3(pk1426)*; Linkage Group III – *ced-4(n1162)*, *ced-4(n2273)*, *ced-9(n2812)*, *daf-2(e1370)*, *daf-2(e1391)*, *daf-2(m596)*; *daf-2(e1370) hpEx792, daf-2(e1370) hpEx791*; Linkage Group IV – *let-60(ga89)*, *let-60(n1046)*; Linkage Group V – *akt-1(ok525)*, *akt-1(ok525); byEx[akt-1::GFP]*, *egl-1(n1084n3082)*; Linkage Group X – *akt-2(ok393)*, *pdk-1(mg142)*, *pdk-1(sa680)*, *pdk-1(sa709)*.

Quantification of germ cell apoptosis. Worms were picked at the L4 stage, aged the desired amount and then subjected to IR from a ^{137}Cs source. After irradiation, all worms were incubated for fixed time/temperature intervals until analysis. For example, we analyzed temperature-sensitive alleles of *daf-2* and *pdk-1* for apoptosis sensitivity at the semi-restrictive temperature of 20°C, the restrictive temperature of 25°C and the permissive temperature of 16°C as indicated in the figure legends. To observe apoptotic cells, worms were mounted on 3–4% agarose pads on glass slides overlaid with a coverslip. 20 mM final concentration of L-tetramisole in M9 buffer was included to paralyze body wall muscles and one germline arm in each animal was observed on a Leica (Wetzlar, Germany) DMRA2 system using standard Differential Interference Contrast optics. Apoptotic cells were distinguished by their characteristic raised and highly refractile morphology. To confirm the apoptotic nature of cells, they were stained with acridine orange, a DNA-binding dye that shows preference for dying cells[45] as described.[11]

Statistical analyses. Statistical significance was determined in Microsoft Excel using a one- or two-sided Student's *t*-test, assuming equal variance.

RNA interference. Worms were fed RNAi from the L1 stage according to the method of Kamath *et al.*[46] Bacterial cultures expressing double-stranded RNA targeting the gene of interest were drawn from the Ahringer library,[47] unless otherwise noted. Control RNAi was drawn from clone *Y95B8A_84.g*, which targets a non-expressed gene.[48] The *daf-2* RNAi clone targeting exon 14 was generated as described.[49]

Quantification of CEP-1/p53 activity. Induction of *egl-1* following irradiation was quantified as described.[11] Data are plotted relative to the wild-type unirradiated control.

Generation of AKT-1 antibodies. Two goat mono-specific polyclonal antisera against *C. elegans* AKT-1 (128 and 527) were generated by Bethyl Laboratories (Montgomery, TX, USA). Peptide antigens corresponded to residues 128–145 (QEELMETNQQPKIDEDSE), which is part of the linker region between the pleckstrin homology and kinase domains of AKT-1, and residues 527–541 (RIHEASEDNEDYDMG), which represents the C terminus of the protein.

Immunoprecipitation and western blotting. Worms of the indicated genotype were synchronized by hypochlorite treatment and grown at 15°C to the L4 stage as described for apoptosis assays. Worms were then irradiated with the indicated dose of IR and incubated for 24 h at 20°C. After washing worms from plates with phosphate-buffered saline (PBS), the pellets were washed once more with PBS and then quickly snap frozen in liquid nitrogen. Approximately 500 μl of Lysis buffer (25 mM Tris (pH 7.4), 1% v/v Triton X-100, 10% v/v glycerol, 150 mM NaCl, 25 mM β-glycerophosphoate, 2 mM phenylmethanesulfonylfluoride) supplemented with Phosphatase Inhibitor Cocktails I and II (Sigma, Oakville, ON, Canada) and Protease Inhibitor Cocktail (Roche, Mississauga, ON, Canada) was added to the worm pellet and sonicated with a Misonix (Farmingdale, NY, USA) 3000 sonicator (power output of 4 for 10 seconds each with ~1 min rest between pulses until the worms were completely lysed). The lysates were then clarified by centrifugation at 13 000 r.p.m. for 10 min at 4°C and the protein content was estimated by Quick Bradford (Pierce, Rockford, IL, USA). A mixture of approximately 2.5 μg each of the two AKT-1 128 and 527 antibodies was used to immunoprecipitate AKT-1 from 0.6–1 mg of total protein (equal amounts of total protein were used in a given experiment) and antigen–antibody complexes were allowed to form overnight at 4°C with rotation. The antigen–antibody complex was subsequently captured with 50 μl of protein-G agarose beads (Upstate, Billerica, MA, USA) for 2 h at 4°C with rotation. Immune complexes bound to beads were washed three times with Lysis buffer supplemented with phosphatase and protease inhibitors and finally boiled in Laemmli sample buffer (0.0625 M Tris (pH 6.8), 2% w/v SDS, 10% v/v glycerol, 5% v/v 2-mercaptoethanol, 0.002% w/v bromophenol blue). Immunoprecipitated proteins were separated by SDS-PAGE on a 10% resolving gel, transferred to polyvinylidene fluoride membranes and blocked in Tris-buffered saline-0.1% v/v Tween-20 (TBST) containing 5% skim milk (T350 and total AKT-1 antibodies) or 5% BSA (S517 antibody). Blots were then probed with rabbit phospho-specific antibodies directed against AKT-1 T350[22] diluted 1 : 1000 in TBST containing 5% BSA, followed by anti-rabbit horseradish peroxidase-conjugated secondary antibodies (1 : 5000 in TBST containing 5% skim milk). After exposure, secondary antibodies were inactivated with 0.1 N HCl and the membrane was reprobed for total AKT-1 using a 1 : 1 mixture of goat AKT-1 antibodies 128 and 527 diluted 1 : 16 000 in TBST containing 5% skim milk, followed by anti-goat horseradish peroxidase-conjugated secondary antibodies (1 : 5000 in TBST containing 5% skim milk). The antibodies were then stripped from the membrane using a 6 M guanidine hydrochloride solution as described.[50] After blocking again in TBST containing 5% BSA, the membrane was probed for S517 phosphorylation using rabbit phospho-specific antibodies targeting AKT-1 S517[22] diluted 1 : 750 in TBST containing 5% BSA. Secondary antibodies were as described for the T350 site. Sometimes, when sufficient protein was isolated, T350 and S517 phosphorylation were analyzed on different membranes by probing each with phospho-specific antibodies first, and then stripping the membrane as described above and finally probing for total AKT-1.

Phospho-MPK-1 staining. Young adult worms (24 h post-L4 stage) were treated with IR as described above and incubated for 24 h at 25°C. Worms were washed from plates with three washes of M9 buffer and the pellet was washed once with 0.01% v/v Tween 20 in M9 and once with ddH_2O. The supernatant was aspirated save ~50 μl and using a pasteur pipette worms were dropped onto slides pre-coated with polylysine. After brief settling, excess liquid was drawn off. Germlines were then dissected from ~50 worms using a 25 gage needle in ~30 μl PBS. PBS was then replaced with ~50 μl of fresh 2% w/v paraformaldehyde and germlines were fixed for 5 min. After fixing, all but ~8 μl of paraformaldehyde was removed and slides were overlaid with a glass coverslip and placed on dry ice (on top of a flat metal plate that had been precooled) for 2–3 min. Coverslips were then 'flicked' off and freeze-cracked germlines were post-fixed for 2 min at −20°C in 50 : 50 mixture of methanol/acetone.

To stain, germlines were permeabilized twice for 10 min with 1% v/v Triton X-100 in PBS. Background staining was reduced by incubating in Image-iT FX Signal Enhancer (Invitrogen, Burlington, ON, Canada) for 20 min at room temperature and then slides were blocked in 1% w/v BSA in PBST for 30 min. Phospho-MPK-1 was detected using α-Phospho-p44/42 MAPK (Cell Signaling Technology, Danvers, MA, USA) diluted 1 : 100 in PBST. Slides were washed three times for 15 min each with PBST, stained with a 1 : 500 dilution of Alexa-conjugated goat α-rabbit and/or 1 : 500 Alexa-conjugated goat α-mouse in PBST plus BSA for 1 h, and then washed a further three times, for 15 min each, with PBST. DNA was stained with 1 μg/ml DAPI in PBST for 15 min and after, slides were washed again with PBST. Slides were then mounted in ProLong Gold (Invitrogen) and visualized using standard epifluorescence filters on a Leica DMRA2 system. Pictures were acquired with a Hamamatsu (Bridgewater, NJ, USA) CCD camera and Openlab software (PerkinElmer, Waltham, MA, USA) before processing in Adobe Photoshop and Illustrator. All staining steps were performed at room temperature, unless otherwise noted.

Conflict of Interest

The authors declare no conflict of interest.

Acknowledgements. We thank members of the Derry Lab for their support and comments on the manuscript, as well as the Kaplan, Irwin and Héon labs for use of equipment. We thank Ashley Ross for assistance in generating strains and Andrew Spence and Brian Ciruna for continuing support. Some nematode strains used in this work were provided by the *Caenorhabditis* Genetics Center, which is funded by the NIH National Center for Research Resources (NCRR). Peter Roy, Ralf Baumeister, Fred Ausubel and Mei Zhen also kindly provided strains and RNAi clones. We thank Anton Gartner for CED-4 and SIR-2.1 antibodies, and Barbara Conradt for CED-9 antibodies. AJP was funded by an MD/ PhD studentship from the

Canadian Institutes of Health Research (CIHR) with additional funding from the Hani family and the Ontario Student Opportunity Trust Fund. WBD is supported by operating grants from the CIHR (MOP102598) and infrastructure grants from the Canada Foundation for Innovation and Ontario Research Fund (Project No. 9782). HAT is a William Randolph Hearst Young Investigator. KY and HAT are funded in part by grants from the National Institute of Aging (AG025891 and AG031237), the Ellison Medical Foundation and an endowment from the William Randolph Hearst Foundation.

1. Vivanco I, Sawyers CL. The phosphatidylinositol 3-Kinase AKT pathway in human cancer. *Nat Rev Cancer* 2002; **2**: 489–501.
2. Liu P, Cheng H, Roberts TM, Zhao JJ. Targeting the phosphoinositide 3-kinase pathway in cancer. *Nat Rev Drug Discov* 2009; **8**: 627–644.
3. Contessa JN, Hampton J, Lammering G, Mikkelsen RB, Dent P, Valerie K *et al.* Ionizing radiation activates Erb-B receptor dependent Akt and p70 S6 kinase signaling in carcinoma cells. *Oncogene* 2002; **21**: 4032–4041.
4. Brognard J, Clark AS, Ni Y, Dennis PA. Akt/protein kinase B is constitutively active in non-small cell lung cancer cells and promotes cellular survival and resistance to chemotherapy and radiation. *Cancer Res* 2001; **61**: 3986–3997.
5. Paradis S, Ailion M, Toker A, Thomas JH, Ruvkun G. A PDK1 homolog is necessary and sufficient to transduce AGE-1 PI3 kinase signals that regulate diapause in Caenorhabditis elegans. *Genes Dev* 1999; **13**: 1438–1452.
6. Paradis S, Ruvkun G. Caenorhabditis elegans Akt/PKB transduces insulin receptor-like signals from AGE-1 PI3 kinase to the DAF-16 transcription factor. *Genes Dev* 1998; **12**: 2488–2498.
7. Lin K, Hsin H, Libina N, Kenyon C. Regulation of the Caenorhabditis elegans longevity protein DAF-16 by insulin/IGF-1 and germline signaling. *Nat Genet* 2001; **28**: 139–145.
8. Lin K, Dorman JB, Rodan A, Kenyon C. daf-16: An HNF-3/forkhead family member that can function to double the life-span of Caenorhabditis elegans. *Science* 1997; **278**: 1319–1322.
9. Ogg S, Paradis S, Gottlieb S, Patterson GI, Lee L, Tissenbaum HA *et al.* The Fork head transcription factor DAF-16 transduces insulin-like metabolic and longevity signals in C. elegans. *Nature* 1997; **389**: 994–999.
10. Lithgow GJ, White TM, Melov S, Johnson TE. Thermotolerance and extended lifespan conferred by single-gene mutations and induced by thermal stress. *Proc Natl Acad Sci U S A* 1995; **92**: 7540–7544.
11. Quevedo C, Kaplan DR, Derry WB. AKT-1 regulates DNA-damage-induced germline apoptosis in C. elegans. *Curr Biol* 2007; **17**: 286–292.
12. Pinkston JM, Garigan D, Hansen M, Kenyon C. Mutations that increase the life span of C. elegans inhibit tumor growth. *Science* 2006; **313**: 971–975.
13. Pinkston-Gosse J, Kenyon C. DAF-16/FOXO targets genes that regulate tumor growth in Caenorhabditis elegans. *Nat Genet* 2007; **39**: 1403–1409.
14. Patel DS, Garza-Garcia A, Nanji M, McElwee JJ, Ackerman D, Driscoll PC *et al.* Clustering of genetically defined allele classes in the Caenorhabditis elegans DAF-2 insulin/IGF-1 receptor. *Genetics* 2008; **178**: 931–946.
15. Ross AJ, Li M, Yu B, Gao MX, Derry WB. The EEL-1 ubiquitin ligase promotes DNA damage-induced germ cell apoptosis in C. elegans. *Cell Death Differ* 2011; **18**: 1140–1149.
16. Ahmed S, Alpi A, Hengartner MO, Gartner A. C. elegans RAD-5/CLK-2 defines a new DNA damage checkpoint protein. *Curr Biol* 2001; **11**: 1934–1944.
17. Ahmed S, Hodgkin J. MRT-2 checkpoint protein is required for germline immortality and telomere replication in C. elegans. *Nature* 2000; **403**: 159–164.
18. Hofmann ER, Milstein S, Boulton SJ, Ye M, Hofmann JJ, Stergiou L *et al.* Caenorhabditis elegans HUS-1 is a DNA damage checkpoint protein required for genome stability and EGL-1-mediated apoptosis. *Curr Biol* 2002; **12**: 1908–1918.
19. Gartner A, Milstein S, Ahmed S, Hodgkin J, Hengartner MO. A conserved checkpoint pathway mediates DNA damage—induced apoptosis and cell cycle arrest in C. elegans. *Mol Cell* 2000; **5**: 435–443.
20. Alessi DR, Andjelkovic M, Caudwell B, Cron P, Morrice N, Cohen P *et al.* Mechanism of activation of protein kinase B by insulin and IGF-1. *EMBO J* 1996; **15**: 6541–6551.
21. Sarbassov DD, Guertin DA, Ali SM, Sabatini DM. Phosphorylation and regulation of Akt/PKB by the rictor-mTOR complex. *Science* 2005; **307**: 1098–1101.
22. Padmanabhan S, Mukhopadhyay A, Narasimhan SD, Tesz G, Czech MP, Tissenbaum HA. A PP2A regulatory subunit regulates C. elegans insulin/IGF-1 signaling by modulating AKT-1 phosphorylation. *Cell* 2009; **136**: 939–951.
23. Kockel L, Kerr KS, Melnick M, Bruckner K, Hebrok M, Perrimon N. Dynamic switch of negative feedback regulation in Drosophila Akt-TOR signaling. *PLoS Genet* 2010; **6**: e1000990.
24. Yan N, Chai J, Lee ES, Gu L, Liu Q, He J *et al.* Structure of the CED-4-CED-9 complex provides insights into programmed cell death in Caenorhabditis elegans. *Nature* 2005; **437**: 831–837.
25. Greiss S, Hall J, Ahmed S, Gartner A. C. elegans SIR-2.1 translocation is linked to a proapoptotic pathway parallel to cep-1/p53 during DNA damage-induced apoptosis. *Genes Dev* 2008; **22**: 2831–2842.
26. Church DL, Guan KL, Lambie EJ. Three genes of the MAP kinase cascade, mek-2, mpk-1/sur-1 and let-60 ras, are required for meiotic cell cycle progression in Caenorhabditis elegans. *Development* 1995; **121**: 2525–2535.
27. Gumienny TL, Lambie E, Hartwieg E, Horvitz HR, Hengartner MO. Genetic control of programmed cell death in the Caenorhabditis elegans hermaphrodite germline. *Development* 1999; **126**: 1011–1022.
28. Kritikou EA, Milstein S, Vidalain PO, Lettre G, Bogan E, Doukoumetzidis K *et al.* C. elegans GLA-3 is a novel component of the MAP kinase MPK-1 signaling pathway required for germ cell survival. *Genes Dev* 2006; **20**: 2279–2292.
29. Rutkowski R, Dickinson R, Stewart G, Craig A, Schimpl M, Keyse SM *et al.* Regulation of Caenorhabditis elegans p53/CEP-1-dependent germ cell apoptosis by Ras/MAPK signaling. *PLoS Genet* 2011; **7**: e1002238.
30. Battu G, Hoier EF, Hajnal A. The C. elegans G-protein-coupled receptor SRA-13 inhibits RAS/MAPK signalling during olfaction and vulval development. *Development* 2003; **130**: 2567–2577.
31. Nanji M, Hopper NA, Gems D. LET-60 RAS modulates effects of insulin/IGF-1 signaling on development and aging in Caenorhabditis elegans. *Aging Cell* 2005; **4**: 235–245.
32. Apfeld J, Kenyon C. Cell nonautonomy of C. elegans daf-2 function in the regulation of diapause and life span. *Cell* 1998; **95**: 199–210.
33. Wolkow CA, Kimura KD, Lee MS, Ruvkun G. Regulation of C. elegans life-span by insulinlike signaling in the nervous system. *Science* 2000; **290**: 147–150.
34. Sijen T, Fleenor J, Simmer F, Thijssen KL, Parrish S, Timmons L *et al.* On the role of RNA amplification in dsRNA-triggered gene silencing. *Cell* 2001; **107**: 465–476.
35. Tijsterman M, Okihara KL, Thijssen K, Plasterk RH. PPW-1, a PAZ/PIWI protein required for efficient germline RNAi, is defective in a natural isolate of C. elegans. *Curr Biol* 2002; **12**: 1535–1540.
36. Ito S, Greiss S, Gartner A, Derry WB. Cell-nonautonomous regulation of C. elegans germ cell death by kri-1. *Curr Biol* 2010; **20**: 333–338.
37. Altun-Gultekin Z, Andachi Y, Tsalik EL, Pilgrim D, Kohara Y, Hobert O. A regulatory cascade of three homeobox genes, ceh-10, ttx-3 and ceh-23, controls cell fate specification of a defined interneuron class in C. elegans. *Development* 2001; **128**: 1951–1969.
38. Evans EA, Chen WC, Tan MW. The DAF-2 insulin-like signaling pathway independently regulates aging and immunity in C. elegans. *Aging Cell* 2008; **7**: 879–893.
39. Gami MS, Iser WB, Hanselman KB, Wolkow CA. Activated AKT/PKB signaling in C. elegans uncouples temporally distinct outputs of DAF-2/insulin-like signaling. *BMC Dev Biol* 2006; **6**: 45.
40. Chalhoub N, Zhu G, Zhu X, Baker SJ. Cell type specificity of PI3K signaling in Pdk1- and Pten-deficient brains. *Genes Dev* 2009; **23**: 1619–1624.
41. Hertweck M, Gobel C, Baumeister R. C. elegans SGK-1 is the critical component in the Akt/PKB kinase complex to control stress response and life span. *Dev Cell* 2004; **6**: 577–588.
42. Vasudevan KM, Barbie DA, Davies MA, Rabinovsky R, McNear CJ, Kim JJ *et al.* AKT-independent signaling downstream of oncogenic PIK3CA mutations in human cancer. *Cancer Cell* 2009; **16**: 21–32.
43. Brognard J, Sierecki E, Gao T, Newton AC. PHLPP and a second isoform, PHLPP2, differentially attenuate the amplitude of Akt signaling by regulating distinct Akt isoforms. *Mol Cell* 2007; **25**: 917–931.
44. Boucher J, Macotela Y, Bezy O, Mori MA, Kriauciunas K, Kahn CR. A kinase-independent role for unoccupied insulin and IGF-1 receptors in the control of apoptosis. *Sci Signal* 2010; **3**: ra87.
45. Abrams JM, White K, Fessler LI, Steller H. Programmed cell death during Drosophila embryogenesis. *Development* 1993; **117**: 29–43.
46. Kamath RS, Martinez-Campos M, Zipperlen P, Fraser AG, Ahringer J. Effectiveness of specific RNA-mediated interference through ingested double-stranded RNA in Caenorhabditis elegans. *Genome Biol* 2001; **2**: Research0002.
47. Kamath RS, Fraser AG, Dong Y, Poulin G, Durbin R, Gotta M *et al.* Systematic functional analysis of the Caenorhabditis elegans genome using RNAi. *Nature* 2003; **421**: 231–237.
48. Lehner B, Crombie C, Tischler J, Fortunato A, Fraser AG. Systematic mapping of genetic interactions in Caenorhabditis elegans identifies common modifiers of diverse signaling pathways. *Nat Genet* 2006; **38**: 896–903.
49. Dixon SJ, Alexander M, Chan KK, Roy PJ. Insulin-like signaling negatively regulates muscle arm extension through DAF-12 in Caenorhabditis elegans. *Dev Biol* 2008; **318**: 153–161.
50. Yeung YG, Stanley ER. A solution for stripping antibodies from polyvinylidene fluoride immunoblots for multiple reprobing. *Anal Biochem* 2009; **389**: 89–91.

Supplementary Information accompanies the paper on Cell Death and Differentiation website (http://www.nature.com/cdd)